Robust Aggregator Design for Industrial Thermal Energy Storages in Smart Grid

Samira Rahnama, Jan Dimon Bendtsen, *Member, IEEE*, Jakob Stoustrup, *Senior Member, IEEE*, and Henrik Rasmussen

***Abstract*—Exploitation of flexible consumption in the future smart grid requires new actors and infrastructure. In this paper, we propose a hierarchical setup in which a central controller, a so-called "aggregator," is responsible for managing the flexibilities of industrial thermal loads via a contract-based direct control policy. The aggregator manipulates the consumption profile in an optimal and robust manner in order to provide upward and downward regulating power services. To this end, we consider a robust model predictive control design at the aggregator. The performance of the proposed controller is evaluated by simulating specific case studies involving a supermarket refrigeration system and a heating, ventilation, and air conditioning chiller in conjunction with an ice storage. In addition, we provide a comparison between heterogeneous and homogeneous aggregation of different thermal loads through simulation examples.**

***Index Terms*—Aggregator, regulating power, robust model predictive control, thermal loads.**

Nomenclature

Indices

j	Index of aggregators.
i	Index of distributed energy resources (DERs).
t	Index of time sample.

Parameters

n	Number of aggregators and number of DERs of each aggregator.
A_{c1}, A_{c2}, B_{c1}, B_{c2}	Constant parameters of the DER continuous-time model.
A_1, A_2, B_1, B_2	Constant parameters of the DER discrete-time model.
α_{c1}, α_{c2}, β_{c1}, β_{c2}	Uncertainty of the continuous-time model parameters.
α_1, α_2, β_1, β_2	Uncertainty of the discrete-time model parameters.
$[\alpha_l^q, \beta_l^q]$ $(l, q = 1, 2)$	Vertices of the uncertainty set.
S_l, R_l, T_l $(l = 1, 2)$	Parameters which define the polytopic sets, $\mathcal{L}_1$ and $\mathcal{L}_2$.
M	Maximum of $S_1x(t) + R_1u(t) - T_1$ inside the polytopic set, $\mathcal{L}$.
m	Minimum of $S_1x(t) + R_1u(t) - T_1$ inside the polytopic set, $\mathcal{L}$.
M_x	Maximum of $x(t)$ inside the polytopic set, $\mathcal{L}$.
m_x	Minimum of $x(t)$ inside the polytopic set, $\mathcal{L}$.
M_u	Maximum of $u(t)$ inside the polytopic set, $\mathcal{L}$.
m_u	Minimum of $u(t)$ inside the polytopic set, $\mathcal{L}$.
$x(t)$	Thermal energy changes of a thermal energy storage (TES).
$u(t)$	Electrical power deviation from the baseline power of a TES.
$\delta(t)$	Auxiliary binary variable to model the logical part of the system.
$z(t)$, $y(t)$	Auxiliary real variables to model the logical part of the system.
P_{ji}	Power reference to the DER "*ji*."
P_j	Power reference to the aggregator *j*.
Φ_j	Profit function of the aggregator *j*.
Ψ_j	Cost function of the aggregator *j*.
$P_{ji,\min}$	Minimum power consumption of the DER *ji*.
$P_{ji,\max}$	Maximum power consumption of the DER *ji*.
$P_{ji,\text{base}}$	Baseline power consumption of the DER *ji*.
$T_{ji,\text{on}}$	On-time period of the DER *ji*.
$T_{ji,\text{off}}$	Off-time period of the DER *ji*.
$P_{\text{reference}}$	Power reference to the top-level controller.

Robust Setup

$X(t)$	Vector of thermal energy changes for a portfolio of n DERs.

Manuscript received February 23, 2015; revised April 11, 2015 and July 23, 2015; accepted September 5, 2015. This work was supported in part by the Danish Government via the Strategic Platform for Innovation and Research in Intelligent Power and iPower, and in part by Aalborg University. Paper no. TSG-00224-2015.

S. Rahnama and J. D. Bendtsen are with the Department of Electronic Systems, Automation, and Control, Aalborg University, Aalborg 9220, Denmark (e-mail: sar@es.aau.dk; dimon@es.aau.dk).

J. Stoustrup is with Pacific Northwest National Laboratory, Richland, WA 99352 USA, and also with the Department of Electronic Systems, Automation, and Control, Aalborg University, Aalborg 9220, Denmark (e-mail: jakob.stoustrup@pnnl.gov).

H. Rasmussen, retired, was with the Department of Electronic Systems, Automation, and Control, Aalborg University, Aalborg 9220, Denmark (e-mail: hgh.rasmussen@gmail.com).

Color versions of one or more of the figures in this paper are available online at http://ieeexplore.ieee.org.

Digital Object Identifier 10.1109/TSG.2015.2481822

$U(t)$	Vector of electrical power deviation from the baseline and the auxiliary variables (z, y, δ) for a portfolio of n DERs.
A, B	Constant matrices of the model parameters for a portfolio of n DERs.
Δ_a, Δ_b	Matrices of parameters' uncertainty for a portfolio of n DERs.
F, G, H	Constant matrices to describe the model constraints for a portfolio of n DERs.
$T_{i,\mathrm{on}}$	On-time period of the DER "i."
$T_{i,\mathrm{off}}$	Off-time period of the DER i.
T_{on}	Maximum of the on-time periods.
T_{off}	Maximum of the off-time periods.
$\mathcal{T}_{i,\mathrm{on}}$	Desired on-time period of the DER i.
$\mathcal{T}_{i,\mathrm{off}}$	Desired off-time period of the DER i.
$\mathcal{X}_{i,\mathrm{act}}$	Desired state of the DER i during the activation time.
$\mathcal{U}_{i,\mathrm{act}}$	Desired input of the DER i during the activation time.
$\mathcal{X}_{i,\mathrm{off}}$	Desired state of the DER "k" during the off-time period.
$\mathcal{U}_{i,\mathrm{off}}$	Desired input of the DER i during the off-time period.
$\mathcal{X}_{i,\mathrm{on}}$	Desired state of the DER i during the on-time period.
$\mathcal{U}_{i,\mathrm{on}}$	Desired input of the DER i during the on-time period.
N_{act}	Number of samples during the activation time.
$N_{i,\mathrm{off}}$	Number of samples during the off-time period for the DER i.
$N_{i,\mathrm{on}}$	Number of samples during the on-time period for the DER i.
N_{off}	Maximum value of $N_{i,\mathrm{off}}$ for $i = 1, \ldots, n$.
N_{on}	Maximum value of $N_{i,\mathrm{on}}$ for $i = 1, \ldots, n$.
N	Number of samples during the extended activation time.
$\mathcal{X}(t)$	Desired value of X.
$\mathcal{U}(t)$	Desired value of U.
Q, R, Γ	Constant weighting matrices.

I. Introduction

THE CURRENT power grid requires a fundamental change in infrastructure to meet the future challenges and to take full advantage of modern technologies. Environmental concerns together with decreasing fossil fuel resources drive many countries to increase the share of renewable energy in power generation. Unlike the traditional resources, wind and solar power are intermittent which necessitate more sophisticated control strategies to stabilize the frequency of power grid [1]. Moreover, the current power grid is changing from the centralized topology to the distributed form with growing use of DERs such as combined heat and power plants, electric vehicles (EVs), etc. This also adds new requirements for congestion management and safe operation of the distribution grid [2]. At the same time, modern sensors and advanced communication technologies enable two-way and automated data exchange between the grid operators, generation side, and intelligent consumers [3]. The future power grid, known as smart grid, utilizes modern technologies and control strategies to overcome the new challenges and consequently, enhance the reliability, efficiency, and sustainability of the power grid [4].

One of the key components of a smart grid is the flexible consumer. In this context, flexible demand refers to those consumers that can advance or postpone their consumption in response to a grid operator command or incentive signal. Utilization of consumers in power management systems, known as demand side management (DSM), is over 40 years old. Generally, DSM programs fall into two categories, demand response (to flatten the demand pattern) and energy efficiency and conservation (to reduce the energy consumption) [5]. Early DSM programs were limited and expensive due to lack of advanced technologies. Smart grid, with the possibility of two-way communication, real-time data exchange and using smart meters and monitoring, facilitates the DSM programs in recent years. There are many works in the literature which have investigated the DSM problems in the smart grid. Some of the works have studied the residential consumption units. For example, home appliances have drawn lots of attention, where the aim is to optimize the energy consumption using smart metering and communication within a home or in a neighborhood level [6]–[8]. DSM at the household levels are not restricted to the home appliances. Building structure can retain the thermal energy, either in the form of warmness or coldness, for a period. The long time constant of the building thermal model can be utilized for load shifting or optimal component operation by manipulating the heating or cooling systems. Not only the building structure, but also external energy storages such as water tank can be used as well. Basically, in these works, advanced control methods such as model predictive control (MPC) are applied which incorporate weather forecast, energy prices, etc. to achieve energy efficient building, i.e., providing a satisfactory comfort level at a lower cost [9]–[12].

However, smart DSM is not only a means of optimizing local energy consumption, but it also facilitates active participation of consumers in the electricity market. The notion of a "smart grid" gives consumers the opportunity to evolve from a mere consumption unit to an active player in the electricity market [13]. It is obvious that the consumers cannot offer in the market individually; since each consumption alone, is not large enough to bid in the market and it is practically impossible to manage from the grid operator point of view. The term "aggregator" has been recently used for a new entity which is in charge of handling the consumer services or their integration to the smart grids [14]. This is a general definition though, and the exact function of the aggregator might be different from case to case. There could be various types of aggregator depending on the control strategy, provided services, type of demand, etc. In general, we can classify the control strategies into two main categories, direct control and indirect control [15]. In summary, in direct control strategies the consumers receive control commands from a grid operator to follow. In most cases, this implies a two-way communication and data exchange between the operator and consumers. On the contrary, indirect control is a one-way communication approach where the grid operator distributes an incentive signal, such as price, to change the consumption, but the consumer independently decides to act on the incentive or not. The aggregator may aim to offer different type of services such as up/down regulation services, primary, secondary and tertiary reserves, voltage control, etc [16]. Finally, various types of consumers ranging from home appliances to industrial enterprises can be aggregated.

For example, aggregation of EVs have been studied in several works, where the aggregator controls the charging process to provide regulation services [17], [18]. Another example is the aggregation of residential thermostatically controlled loads (TCLs) such as water heaters, refrigerators, air conditioners, etc. For instance, Sanandaji *et al.* [19] investigated the aggregation of TCLs to provide fast regulation services (seconds to 1 min time scale). Other example for the TCLs aggregation can be found in [20]–[22]. A general market model for residential demand response in smart grid is given in [23]. Literature review regarding the aggregator design reveals that most of the works are dedicated to small energy consumers, whereas the works on industrial consumers are rather limited. As an example, Vrettos *et al.* [24] proposed a hierarchical control scheme to aggregate the heating, ventilation, and air conditioning (HVAC) systems of commercial buildings for secondary frequency control provision. Similar work for the aggregation of HVAC units to follow the regulation and load following signals is given in [25].

In [26], we proposed an aggregator setup with the following features.

1) We have chosen industrial consumers which is less addressed in the literature. A few of industrial enterprises are large enough to bid in the electricity market. Thus, we can implement a central aggregator which has the consumers under its direct jurisdiction in practice. Moreover, industrial consumers have less privacy issues compared to the households. This facilitates the information exchange between the consumers and the aggregator which is necessary for the proposed setup.
2) Such aggregator operates in a three-level hierarchical structure consists of three levels, a top-level controller that can be located at the transmission system operator (TSO), distribution system operator (DSO), or balance responsible party (BRP), an aggregator in the middle and a number of consumers at the bottom. We consider a power reference following scenario as follows: "the aggregator and the grid operator sign a contract which allows the grid operator to activate the aggregator for a certain period of time, called the activation time. The aggregator is asked to follow a specified power reference within the activation time." The power reference following service can be of interest to any grid operator in the electricity market. For instance, in the current Nordic electricity market, BRPs are trading companies, which have the responsibility of supplying energy to a number of consumers under their jurisdiction during a given period of time. They trade power in different markets. For example, in the day-ahead market, BRPs bid their power schedules a day before the actual consumption/production based on the anticipated consumption. By utilizing the flexibility of consumers, BRPs will be able to reduce the cost of deviation between the power which is bought/sold one day ahead and the actual consumption/production. In other words, the actual consumption is becoming closer to anticipated consumption. TSO is a noncommercial organization, which is responsible for reliable and secure operation of the whole power grid. To maintain the balance continuously, TSO should provide regulating powers as upward and downward regulation, meaning increase and decrease in production, respectively. The proposed aggregator can bid in the regulating power market by providing upward and downward regulating power with decreasing and increasing the consumption instead. At the low-voltage level, DSOs are responsible for the physical grid, here, avoiding congestion and controlling the voltage level of the feeders are the main issues. The power reference following service can ensure the DSO that a feeder of interest will never be higher loaded than specified by the DSO.
3) The aggregator optimizes the power distribution for two cases: a) when the power reference is greater than the aggregated baseline consumption; and b) when it is lower.
4) In the proposed setup, we deliberately used simplified models of the consumers at the aggregator, even though the physical systems are known to be more complicated. Otherwise, the setup is not applicable in practice. To compensate for the deviation arising from the model mismatch, we considered a simple feedback mechanism in which we represented the discrepancies as state-dependent uncertainties. We then redistributed the discrepancies among the consumers.

In this paper, we first generalize the hierarchical setup by considering a number of aggregators and explain the interplay between the aggregators and the top-level controller. Rather than assuming a specific case study for the aggregator design, same as [24] and [25], our proposed aggregator design can be applied to any large-scale thermal load. For simulation example, we choose the supermarket refrigeration system and the HVAC chiller connected to an ice tank. Though the simulations, we provide a comparison between the heterogeneous and homogeneous aggregation. As the main contribution of this paper, instead of the aforementioned feedback mechanism, we include the uncertainties inside the controller at the aggregator. This approach leads to a robust MPC framework in which the model structure is known. However, the model parameters are allowed to vary within a predefined convex set.

The rest of this paper is organized as follows. In Section II, we illustrate the general setup including the heterogeneous and homogeneous framework and interaction between the players. In Section III, we present the robust MPC design. In Section IV, simulation results are provided. We consider two simulation scenarios. One scenario is related to the comparison of heterogeneous versus homogeneous aggregation. In the other scenario, we investigate the performance of the proposed

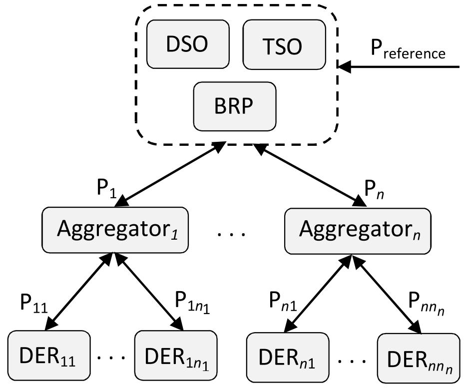

Fig. 1. Three-level hierarchical aggregation setup. $\text{DER}_{ji}(j = 1, \dots, n$ $i = 1, \dots, n_j)$ stands for the ith DER belonging to the aggregator j. P_j and P_{ji} are the power references.

robust MPC. In Section V, we conclude this paper. Note that throughout this paper, all symbols represent real scalars, unless specifically stated.

II. General Setup

A. Heterogeneous Versus Homogeneous Aggregation

The general hierarchical setup is depicted in Fig. 1. It consists of a top-level controller that can be located at BRP, TSO, or DSO, a number of aggregators in the middle and a number of flexible thermal loads, which can be seen as DERs under the control of each aggregator at the bottom. In the homogeneous setup, each aggregator is connected to the DERs of a same type, while in the heterogeneous aggregation, the aggregator utilizes the flexibility of DERs with different flexibility characteristics.

B. Model of Consumers

In this paper, we solely focus on a specific class of flexible consumers; TESs. Excess electrical energy can be stored in form of thermal energy in TESs for later use in the future. In modeling a TES, we aim to represent the thermal energy changes that result from input excess/shortage of electrical power. Thus, we define the system state, $x \in \mathbb{R}$, and the system input, $u \in \mathbb{R}$, as below.

1) $x(t) \triangleq$ thermal energy changes from the baseline.
2) $u(t) \triangleq$ electrical power deviation from the baseline power.

In order to avoid complex notation, we omit the subscript ji from all the variables in this section. We look at the whole consumption unit as a lump TES. As stated above, a simplified model of the real complicated system can be utilized at the aggregator for our purpose. Simulation results in [27] also reveal that a first order model can reasonably approximate the behavior of a supermarket refrigeration system as an example of a TES. Assume $\begin{bmatrix} x \\ u \end{bmatrix} \in \mathcal{L}$, where $\mathcal{L} \subset \mathbb{R} \times \mathbb{R}$ is a polytopic set. Then, the general model of a TES is expressed by (1)–(3). We consider a piece-wise linear dynamic system including two separate linear models. In this way, we can explain those systems which are operated in two different modes with significant difference between the system parameters. For instance, the system dynamics might vary significantly from day-time to night-time because of coefficient of performance (COP) effects. Another example could be the two separate modes (ice-making and direct cooling) in cooling and air conditioning systems. Instead of increasing the number of models, small changes in system parameters are modeled by considering uncertain parameters in each mode. Note that we consider multiplicative uncertainties

$$\dot{x}(t) = \begin{cases} (A_{c1} + \alpha_{c1})x(t) + (B_{c1} + \beta_{c1})u(t) & \text{if } \begin{bmatrix} x \\ u \end{bmatrix} \in \mathcal{L}_1 \\ (A_{c2} + \alpha_{c2})x(t) + (B_{c2} + \beta_{c2})u(t) & \text{if } \begin{bmatrix} x \\ u \end{bmatrix} \in \mathcal{L}_2 \end{cases} \tag{1}$$

$$\mathcal{L}_1 \bigcap \mathcal{L}_2 = \emptyset,\ \mathcal{L}_1 \bigcup \mathcal{L}_2 = \mathcal{L} \tag{2}$$

$$\mathcal{L}_l = \left\{ \begin{bmatrix} x \\ u \end{bmatrix} : S_l x + R_l u \leq T_l \right\}, \quad l = 1, 2 \tag{3}$$

where $A_{c1}, A_{c2}, B_{c1}, B_{c2} \in \mathbb{R}$ are known parameters of the continuous model and the sets $\mathcal{L}_l$ are polytopes defined by $S_l, R_l, T_l \in \mathbb{R}$. The corresponding discrete-time system is given in (4). A polytopic uncertainty set is assumed as shown in (5), where Co denotes the convex hull and $[\alpha_l^q, \beta_l^q]$ $(l, q = 1, 2)$ are vertices of the uncertainty set

$$x(t+1) = \begin{cases} (A_1 + \alpha_1)x(t) + (B_1 + \beta_1)u(t) & \text{if } \begin{bmatrix} x \\ u \end{bmatrix} \in \mathcal{L}_1 \\ (A_2 + \alpha_2)x(t) + (B_2 + \beta_2)u(t) & \text{if } \begin{bmatrix} x \\ u \end{bmatrix} \in \mathcal{L}_2 \end{cases} \tag{4}$$

$$[\alpha_l, \beta_l] \in \text{Co}\left\{ \left[\alpha_l^1, \beta_l^1\right], \left[\alpha_l^2, \beta_l^2\right] \right\}, \quad l = 1, 2. \tag{5}$$

To model the logical part of the system, we define an auxiliary binary variable, $\delta(t) \in \{0, 1\}$ such that (6) holds

$$\begin{bmatrix} x \\ u \end{bmatrix} \in \mathcal{L}_1 \Longleftrightarrow \delta(t) = 1. \tag{6}$$

Moreover, two auxiliary real variables, $z(t)$ and $y(t)$, are needed as (7) and (8). Thereafter, the system dynamics can be represented as follows:

$$z(t) \triangleq x(t)\delta(t) \tag{7}$$

$$y(t) \triangleq u(t)\delta(t) \tag{8}$$

$$\begin{aligned} x(t+1) = {} & (A_2 + \alpha_2)x(t) + (B_2 + \beta_2)u(t) \\ & + (A_1 + \alpha_1 - A_2 - \alpha_2)z(t) \\ & + (B_1 + \beta_1 - B_2 - \beta_2)y(t). \end{aligned} \tag{9}$$

Equation (6) cannot be directly used in the optimization problem and (7) and (8) are also products between the two decision variables. We use the techniques proposed in [28] to convert these equations to mixed-integer linear inequalities. Equation (6) can be replaced by inequalities (10)–(13) and (7)–(8) can be replaced as follows:

$$S_1 x(t) + R_1 u(t) - T_1 \leq M(1 - \delta(t)) \tag{10}$$

$$S_1 x(t) + R_1 u(t) - T_1 \geq \epsilon + (m - \epsilon)\delta(t) \tag{11}$$

$$M \triangleq \max_{[x,u]\in\mathcal{L}}\{S_1x(t)+R_1u(t)-T_1\} \tag{12}$$

$$m \triangleq \min_{[x,u]\in\mathcal{L}}\{S_1x(t)+R_1u(t)-T_1\} \tag{13}$$

$$z(t) \le M_x\delta(t) \tag{14}$$

$$z(t) \ge m_x\delta(t) \tag{15}$$

$$y(t) \le M_u\delta(t) \tag{16}$$

$$y(t) \ge m_u\delta(t) \tag{17}$$

$$z(t) \le x(t)-m_x(1-\delta(t)) \tag{18}$$

$$z(t) \ge x(t)-M_x(1-\delta(t)) \tag{19}$$

$$y(t) \le u(t)-m_u(1-\delta(t)) \tag{20}$$

$$y(t) \ge u(t)-M_u(1-\delta(t)) \tag{21}$$

$$M_x \triangleq \max_{x\in\mathcal{L}}\{x\} \tag{22}$$

$$m_x \triangleq \min_{x\in\mathcal{L}}\{x\} \tag{23}$$

$$M_u \triangleq \max_{u\in\mathcal{L}}\{u\} \tag{24}$$

$$m_u \triangleq \min_{u\in\mathcal{L}}\{u\}. \tag{25}$$

Furthermore, each dynamical system is subject to physical constraints. Thus, we need to consider the input and state constraints as

$$u_{\min} \le u(t) \le u_{\max} \tag{26}$$

$$x_{\min} \le x(t) \le x_{\max}. \tag{27}$$

In the model presented above, we assume the system input can be changed continuously. ϵ is a small positive number in the above equations.

This model is sufficient to describe the salient features of a TES. Various types of TESs are distinguished by the following key features: 1) leakiness, i.e., loss during storage; 2) efficiency in conversion; 3) power capacity; and 4) energy capacity.

Fig. 2 depicts the salient features of such a simplified thermal storage. The parameters $(A_1+\alpha_1)$ and $(A_2+\alpha_2)$ specify whether the TES is leaky or not in each operation mode. Efficiency in conversion (from electrical to thermal power) or the COP of the system is reflected in $(B_1+\beta_1)$ and $(B_2+\beta_2)$. Power and energy capacity are defined with input and state constraints as (26) and (27). We can list more features in addition to the aforementioned features. For instance, there may be other constraints in addition to the power and energy constraints in the process of energy conversion such as pressure constraints, etc. However, the aggregator is not responsible for controlling the consumers in detail, such as every single pump or valve. These are the responsibilities of local controller. Thus, it is not necessary to have complex models at the aggregator.

C. Objective Function

The objective of the setup shown in Fig. 1 is as follows: "the top-level controller aims to keep the power consumption of the whole portfolio at a specified level, $P_{\text{reference}}$, during a specific activation time." To meet the objective, the interactions between the top-level controller and the aggregators and also between one aggregator and the consumers at its disposal, should be determined. The latter is explained in detail in [26]. Here, we provide a brief summary together with the first interaction. Assume P_j and P_{ji} ($j = 1,\ldots,n$ and $i = 1,\ldots,n_j$) denote the power references from the top-level controller to the aggregators and from the aggregators to the consumers, respectively. Under normal circumstances, when there is no activation, consumers consume the amount of power they require to run their systems in the optimal manner defined by the local controller. This power is called the baseline power. To formulate the objective function at the aggregator, we consider two general cases, when the power flow to the aggregator is above its aggregated baseline consumption (down-regulation) and when it is below (up-regulation). First, let us consider the down-regulating scenario. During the down-regulation activation time, the total consumption is above the aggregated baseline power. In this situation, the aggregator has the chance to save some extra energy in its thermal storages during the activation. Right after the activation, the aggregator can benefit from this saving by using the stored energy and lowering its consumption to under baseline consumption. Thus, the optimal is to retrieve as much energy as we can after the activation. The objective function at the aggregator j for the down-regulating scenario is formulated as

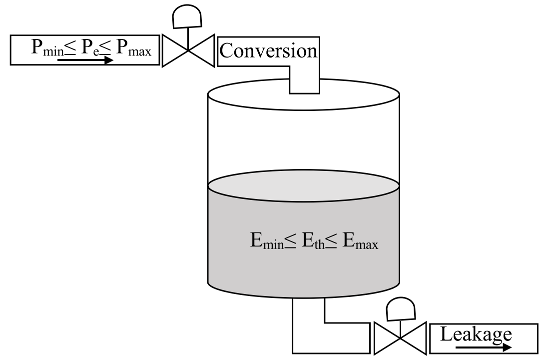

Fig. 2. Salient features of a thermal storage.

$$\max_{u_{ji},z_{ji},y_{ji},\delta_{ji}(i=1,2,\ldots,n_j)} \quad \Phi_j = \sum_{i=1}^{n_j}\left(P_{ji,\text{base}}-P_{ji,\min}\right)T_{ji,\text{off}} \tag{28}$$

$$P_{j1}+P_{j2}+\cdots+P_{jn_j} = P_j \tag{29}$$

$$(9)\text{–}(11),\ (14)\text{–}(21),\ (26),\ (27)$$

where $T_{ji,\text{off}}$ (off-time period) represents the period after the activation when the consumer decreases its consumption from the baseline, $P_{ji,\text{base}}$, to the minimum level, $P_{ji,\min}$. In case of no activation, the consumer needs to consume at least the baseline consumption during this period. Thus, the consumer is able to save power corresponding to $P_{ji,\text{base}}-P_{ji,\min}$ at each time instant during $T_{ij,\text{off}}$. In fact, Φ_j is the energy saving after the activation. Reducing the power consumption to the minimum level minimizes the time needed for regaining the stored energy and consequently minimizes the heat loss to the surrounding. In other words, it is optimal to deplete the energy as fast as possible to minimize the loss. The problem in the up-regulating scenario is symmetric to the down-regulation. During the up-regulation activation time, the total consumption is below the aggregated baseline power. In this case, the aggregator needs to store some energy before the activation in order to deliver it during the activation time. The objective function at the aggregator j for the up-regulating scenario is formulated as

$$\min_{u_{ji},z_{ji},y_{ji},\delta_{ji}(i=1,2,\ldots,n_j)} \quad \Psi_j = \sum_{i=1}^{n_j}\left(P_{ji,\max} - P_{ji,\mathrm{base}}\right)T_{ji,\mathrm{on}} \tag{30}$$

$$P_{j1} + P_{j2} + \cdots + P_{jn_j} = P_j \tag{31}$$

$$(9)\text{–}(11),\ (14)\text{–}(21),\ (26),\ (27)$$

where $T_{ji,\mathrm{on}}$ (on-time period) is the period before the activation when the consumer increases its consumption from the baseline to the maximum level, $P_{ji,\max}$ to store the required energy. The consumer has to consume $P_{ji,\max} - P_{ji,\mathrm{base}}$ more than its normal operation at each time instant during $T_{ji,\mathrm{on}}$. Ψ_j is the cost, in terms of energy consumption, that should be paid by the aggregator. Similar to the first case, it is better to save the energy as fast as possible during the $T_{ji,\mathrm{on}}$ to minimize the loss. That is why the consumer consumes its maximum power before the activation. In above optimizations, $u_{ji} = P_{ji} - P_{ji,\mathrm{base}}$.

In the hierarchical setup shown in Fig. 1, we assume several aggregators and the grid operator aims to provide $P_{\mathrm{reference}}$ from all of them. Therefore, a question arises: how the power distribution from the grid operator to the aggregators should be, where there are different aggregators with different capacities and costs. For this level, we consider a one-time optimization. The mechanism is as follows. Each aggregator communicates the cost (Ψ_j)/profit (Φ_j) curves to the grid operator which illustrate the cost/profit, in terms of energy, per a specified power reference. Based on this information, the top-level controller performs a one-time optimization to produce $P_1, P_2, \ldots, P_n$

$$\min_{P_1,\ldots,P_n} \quad \sum_{j=1}^{n} \Psi_j \quad \text{(up-regulation)} \tag{32}$$

$$\max_{P_1,\ldots,P_n} \quad \sum_{j=1}^{n} \Phi_j \quad \text{(down-regulation)} \tag{33}$$

$$\text{subject to:} \quad P_1 + P_2 + \cdots + P_n = P_{\mathrm{reference}} \tag{34}$$

$$P_{j,\min} \le P_j \le P_{j,\max} \quad (j = 1, \ldots, n) \tag{35}$$

where $P_{j,\min}$ and $P_{j,\max}$ are the minimum and maximum power consumption of the total consumers controlled by "Aggregator j." These power flows $(P_1, \ldots, P_n)$ will be fixed during the activation period.

III. Robust MPC on Aggregator Level

A. Model With Uncertainties and Constraints

In this section, we assume only one aggregator which has n TESs ($i = 1, \ldots, n$) under its control. For the sake of simplicity, we delete the index j related to the aggregators. Each consumer has the following model:

$$x_i(t+1) = \begin{cases} (A_{i,1} + \alpha_{i,1})x_i(t) \\ \qquad + (B_{i,1} + \beta_{i,1})u_i(t) & \begin{bmatrix} x_i \\ u_i \end{bmatrix} \in \mathcal{L}_{i,1} \\ (A_{i,2} + \alpha_{i,2})x_i(t) \\ \qquad + (B_{i,2} + \beta_{i,2})u_i(t) & \begin{bmatrix} x_i \\ u_i \end{bmatrix} \in \mathcal{L}_{i,2}. \end{cases} \tag{36}$$

Thus, the model of the whole portfolio is as follows:

$$\begin{aligned} X(t+1) &= (A + \Delta_a)X(t) + (B + \Delta_b)U(t) \\ X(t) &\triangleq [x_1(t) \ \ldots \ x_n(t)]^T \\ U(t) &\triangleq [u_1(t)\ z_1(t)\ y_1(t)\ \delta_1(t) \ldots u_n(t)\ z_n(t)\ y_n(t)\ \delta_n(t)]^T \\ A &\triangleq \begin{bmatrix} A_{1,2} & & 0 \\ & \ddots & \\ 0 & & A_{n,2} \end{bmatrix}_{n\times n} \quad \Delta_a \triangleq \begin{bmatrix} \alpha_{1,2} & & 0 \\ & \ddots & \\ 0 & & \alpha_{n,2} \end{bmatrix}_{n\times n} \\ B &\triangleq \begin{bmatrix} \boldsymbol{B}_{1,2} & & 0 \\ & \ddots & \\ 0 & & \boldsymbol{B}_{n,2} \end{bmatrix}_{n\times 4n} \quad \Delta_b \triangleq \begin{bmatrix} \boldsymbol{\beta}_{1,2} & & 0 \\ & \ddots & \\ 0 & & \boldsymbol{\beta}_{n,2} \end{bmatrix}_{n\times 4n} \\ \boldsymbol{B}_{i,2} &\triangleq [B_{i,2} \quad A_{i,1} - A_{i,2} \quad B_{i,1} - B_{i,2} \quad 0] \\ \boldsymbol{\beta}_{i,2} &\triangleq [\beta_{i,2} \quad \alpha_{i,1} - \alpha_{i,2} \quad \beta_{i,1} - \beta_{i,2} \quad 0] \quad (i = 1, \ldots, n) \end{aligned} \tag{37}$$

and the model is subject to mixed constraints in which both physical constraints (26) and (27) and constraints related to the mixed logical models (10), (11), and (14)–(21) are included

$$FX(t) + GU(t) \le H \tag{38}$$

where $F \in \mathbb{R}^{14n\times n}$, $G \in \mathbb{R}^{14n\times 4n}$, and $H \in \mathbb{R}^{14n}$ are constant matrices with appropriate dimensions, related to the above-mentioned constraints for n units plus the power reference following equation.

B. Control Formulation

In Section II, the objective function at the aggregator level has been formulated for the up/down-regulation scenarios. The proposed objective functions rely on the off-time and on-time periods of the consumers. In general, for each TES, off-time and on-time periods are nonlinear functions of the state of the charge at the end and at the beginning of the activation, respectively. For the piece-wise linear dynamic (1), the function is a logarithmic function whose parameters can vary depending on the set definitions, $\mathcal{L}_1$ and $\mathcal{L}_2$. For example, in a special case, when $S_1 = T_1 = S_2 = T_2 = 0$, $R_1 = -1$, and $R_2 = 1$, they can be obtained as below for the consumer i

$$T_{i,\mathrm{off}} = \frac{-1}{A_{i,c1} + \alpha_{i,c1}} \ln\left(1 - \frac{(A_{i,c1} + \alpha_{i,c1})x_i(N_{\mathrm{act}})}{(B_{i,c1} + \beta_{i,c1})(P_{i,\mathrm{base}} - P_{i,\min})}\right) \tag{39}$$

$$T_{i,\mathrm{on}} = \frac{1}{A_{i,c2} + \alpha_{i,c2}} \ln\left(1 + \frac{(A_{i,c2} + \alpha_{i,c2})x_i(1)}{(B_{i,c2} + \beta_{i,c2})(P_{i,\max} - P_{i,\mathrm{base}})}\right) \tag{40}$$

where $x_i(N_{\mathrm{act}})$ and $x_i(1)$ are the state of the charge of the systems at the end and at the beginning of the activation time. N_{act} is the number of samples during the activation time. $T_{i,\mathrm{off}}$

is the time after the activation time which takes to fully deplete the stored energy at the end of the activation time for the TES i. $T_{i,\text{on}}$ is the time before the activation time which takes to store the required energy at the beginning of the activation time for the TES i. Based on these definitions, (39) and (40) are obtained, considering the fact that the solution of the first order linear model has the exponential form.

To apply a robust algorithm at the aggregator level in a real time situation, we propose a two-step strategy. The first step is performed long before the activation time. The aggregator solves a one-time optimization problem using the objective functions (28) and (30). In the second step, based on the information obtained from the first step, the aggregator solves an optimization problem every sampling time during the extended activation time. The extended activation time refers to the activation time, when the units are required to follow the power reference, plus the on-time or the off-time periods. In the following, we will explain each step in details.

1) For the down-regulating scenario, the aggregator performs a profit optimization to maximize the profit function as formulated in equation (41)

$$\max_{u_i,z_i,y_i,\delta_i(i=1,\dots,n)} \quad \sum_{i=1}^{n}(P_{i,\text{base}} - P_{i,\text{min}}) \times T_{i,\text{off}}. \tag{41}$$

In this optimization, the aggregator uses those system parameters, within the uncertainty set, which produces the maximum profit. Since the profit function is a function of $T_{i,\text{off}}$, then the aggregator should use the system parameters which produces the maximum $T_{i,\text{off}}$ for $i = 1, \dots, n$. Analytically, it is not straightforward to say which parameters will generate the maximum profit. For example, for the special case in (39), $T_{i,\text{off}}$ decreases with the increase in $\beta_{i,c1}$ at first glance. However, $x_i(N_{\text{act}})$ also increases with the increase in $\beta_{i,c1}$, since it is dependent on $\beta_{i,c1}$. Moreover, off-time period for one system is also dependent on off-time period of the other systems and we are interested in maximizing the total profit. Nevertheless, as we explained in Section II, we know the physical interpretation of the system parameters. A_{c1} and B_{c1} model the heat loss and efficiency in conversion (COP) of a TES, respectively. Thus, the greater α_{c1} and β_{c1} we have, the more profit we achieve. In other words,

$$\begin{aligned}\forall[\alpha_{i,c1}, \beta_{i,c1}] \in \text{Co}\Big\{\big[\alpha_{i,c1}^1, \beta_{i,c1}^1\big], \big[\alpha_{i,c1}^2, \beta_{i,c1}^2\big]\Big\}\\ \Phi \le \Phi|_{\max\{\alpha_{i,c1}\},\max\{\beta_{i,c1}\}} \quad (i = 1, \dots, n).\end{aligned} \tag{42}$$

For the up-regulating scenario, the aggregator performs a cost optimization as follows:

$$\min_{u_i,z_i,y_i,\delta_i(i=1,\dots,n)} \sum_{i=1}^{n}(P_{i,\max} - P_{i,\text{base}}) \times T_{i,\text{on}}. \tag{43}$$

In this scenario, the aggregator uses those system parameters, within the uncertainty set, which provide the maximum cost. With the same argument as the down-regulating scenario, we can say the maximum cost is achieved for the minimum α_{c2} and β_{c2}. Thus, the below statement should hold

$$\begin{aligned}\forall[\alpha_{i,c2}, \beta_{i,c2}] \in \text{Co}\Big\{\big[\alpha_{i,c2}^1, \beta_{i,c2}^1\big], \big[\alpha_{i,c2}^2, \beta_{i,c2}^2\big]\Big\}\\ \Psi \le \Psi|_{\min\{\alpha_{i,c2}\},\min\{\beta_{i,c2}\}} \quad (i = 1, \dots, n).\end{aligned} \tag{44}$$

Let us denote the optimum state and input sequences obtained from the optimizations (41) and (43) by $\{\mathcal{X}_{i,\text{act}}(t)\}_{t=1}^{t=N_{\text{act}}}$ and $\{\mathcal{U}_{i,\text{act}}(t)\}_{t=1}^{t=N_{\text{act}}}$. The optimizations also generate the optimum values of off-time and on-time periods for each consumer: $\mathcal{T}_{i,\text{off}}$ and $\mathcal{T}_{i,\text{on}}$, when the consumers consume the minimum and maximum power, respectively. Thus, during the off-time and on-time periods, the system inputs are

$$\big\{\mathcal{U}_{i,\text{off}}(t) = P_{i,\min} - P_{i,\text{base}}\big\}_{t=1}^{t=N_{i,\text{off}}} \tag{45}$$

$$\big\{\mathcal{U}_{i,\text{on}}(t) = P_{i,\max} - P_{i,\text{base}}\big\}_{t=1}^{t=N_{i,\text{on}}} \tag{46}$$

where $N_{i,\text{off}}$ and $N_{i,\text{on}}$ are the number of samples during the off-time and on-time periods corresponding to each consumer, i. Hereupon, we have $\{\mathcal{X}_{i,\text{off}}(t)\}_{t=1}^{t=N_{i,\text{off}}}$ and $\{\mathcal{X}_{i,\text{on}}(t)\}_{t=1}^{t=N_{i,\text{on}}}$. Afterwards, we construct the following vectors:

up-regulating

$$\mathcal{X}_i \triangleq \big[0_{1\times(N_{\text{on}}-N_{i,\text{on}})} \quad \mathcal{X}_{i,\text{on}}(1:N_{i,\text{on}}) \quad \mathcal{X}_{i,\text{act}}(1:N_{\text{act}})\big] \tag{47}$$

$$\mathcal{U}_i \triangleq \big[0_{1\times(N_{\text{on}}-N_{i,\text{on}})} \quad \mathcal{U}_{i,\text{on}}(1:N_{i,\text{on}}) \quad \mathcal{U}_{i,\text{act}}(1:N_{\text{act}})\big] \tag{48}$$

down-regulating

$$\mathcal{X}_i \triangleq \big[\mathcal{X}_{i,\text{act}}(1:N_{\text{act}}) \quad \mathcal{X}_{i,\text{off}}(1:N_{i,\text{off}}) \quad 0_{1\times(N_{\text{off}}-N_{i,\text{off}})}\big] \tag{49}$$

$$\mathcal{U}_i \triangleq \big[\mathcal{U}_{i,\text{act}}(1:N_{\text{act}}) \quad \mathcal{U}_{i,\text{off}}(1:N_{i,\text{off}}) \quad 0_{1\times(N_{\text{off}}-N_{i,\text{off}})}\big] \tag{50}$$

where each vector has the length of N. $N = N_{\text{act}} + N_{\text{on}}$ and $N = N_{\text{act}} + N_{\text{off}}$ for up-regulating and down-regulating, respectively. Each consumer has its own on-time and off-time periods. We choose the maximum value among the whole portfolio. Hence, $N_{\text{on}} = \max_i\{N_{i,\text{on}}\}$ and $N_{\text{off}} = \max_i\{N_{i,\text{off}}\}$ $(i = 1, \dots, n)$. The rest of the vector is filled up with zeros. Fig. 3 shows a typical power consumption profile and the stored thermal energy of a consumer for up-regulating and down-regulating scenarios. t_{start} and t_{end} denote the beginning and end of activation time when the consumers need to follow a time-varying power reference. This time is extended with on and off-time periods when the consumers receive a constant power reference. Outside of this region, each consumer consumes its baseline power, which is optimal from the local controller's point of view. Here, we assume the baseline consumption is constant. In practice, the time-varying baseline consumption can be communicated to the aggregator during the service activation.

2) During the time of service activation, the aggregator runs the optimization with the quadratic cost function as formulated in equation (51) every sampling time

$$\begin{aligned}\min_{U} \quad & \sum_{t=1}^{N}(X(t) - \mathcal{X}(t))^T Q(X(t) - \mathcal{X}(t))\\ & + (\Gamma U(t) - \mathcal{U}(t))^T R(\Gamma U(t) - \mathcal{U}(t)) \qquad (51)\\ \text{subject to:} \quad & \sum \Gamma U(t) = u_{\text{reference}} \ (t_{\text{start}} \le t \le t_{\text{end}})\\ & (37),\ (38) \qquad (52)\end{aligned}$$

where $\mathcal{X}(t) = [\mathcal{X}_1(t) \dots \mathcal{X}_n(t)]^T$ and $\mathcal{U}(t) = [\mathcal{U}_1(t) \dots \mathcal{U}_n(t)]^T$. $Q \in \mathbb{R}^{n\times n}$ and $R \in \mathbb{R}^{n\times n}$ are constant weighting matrices. $\Gamma \in \mathbb{R}^{n\times 4n}$ is a matrix with 0 and 1 elements used

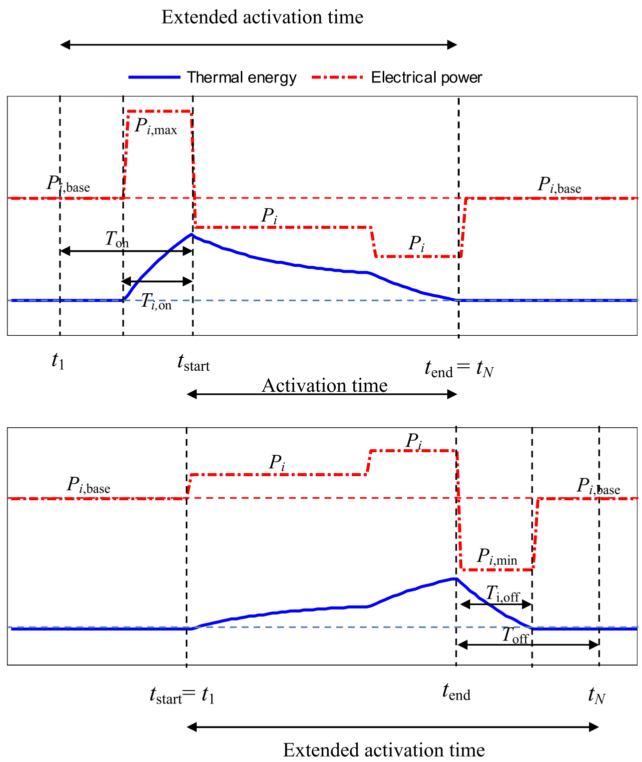

Fig. 3. Typical power consumption profile and the stored thermal energy of a consumer i for up-regulating (top) and down-regulating (bottom). $[t_{\text{start}}, t_{\text{end}}]$ denote the activation time, whereas $[t_1, t_N]$ indicates the prediction horizon in the second step. T_{on} and T_{off} are the maximum on-time and off-time periods among the whole portfolio.

for converting U to u. N is the prediction horizon for the MPC. The above optimization starts at t_1 and finishes at t_N. At each sampling time, the optimization provides the optimum input for the whole prediction horizon and only the first element is applied to the system. At the first sampling time t_1, $\mathcal{U}(t)$ and $\mathcal{X}(t)$ are available for $t = 1, \ldots, N$ from the optimization in the first step. As we proceed, we need to update them every sampling time by eliminating the first element and adding zero to the end. For instance, at $t_1 + \tau$ (τ is the sampling time), $\mathcal{U}(N) = \mathcal{X}(N) = \mathbf{0}_{n\times 1}$, at $t_1 + 2\tau$, $\mathcal{U}(N-1:N) = \mathcal{X}(N-1:N) = \mathbf{0}_{n\times 2}$ and so on. Equation (52) represents power reference following. In (37), we use the minimum value of Δ_a and Δ_b for up-regulating scenario and we use the maximum value of Δ_a and Δ_b for down-regulating scenario. If the real system parameters are different from these in the time of service activation, we can expect the following output: in the up-regulating scenario, the aggregator might ask some of the units to consume less than their maximum power consumption during the on-time period. In the down-regulating scenario, some of the units might consume greater than their minimum consumption during the off-time period. However, in both cases, the aggregator can follow the power reference during the activation time.

IV. Simulation Examples

Two specific case studies are selected for simulation: 1) supermarket refrigeration systems; and 2) chillers in air conditioning systems. For the first one, cold rooms and display cases can act as a thermal storage where we store energy in refrigerated foods. For the second one, an ice storage connected to the chiller serves as a thermal storage. In [27], we presented appropriate models of these consumer types for optimization purposes. In brief, cold rooms and display cases at the supermarket can be seen as a thermal storage with a leakage because of heat load from the surrounding, whereas an ice tank is a storage with no leakage, since it is well-isolated. We assumed constant COP for the supermarket. For the chiller, we assumed two constant COPs associated with direct cooling and charging modes. The chiller is operated in charging mode when the input power is above the baseline power. Thus, the extra power is used to make ice. When the input power is below the baseline, part of the cooling load is provided by melting the ice. In this situation, the chiller is utilized in conjunction with the ice tank in direct cooling mode. To compare the heterogeneous and homogeneous setup, we consider two supermarkets and two chillers. All in all, the following equations describe the model of the consumers:

Supermarket 1

$$x_1(t+1) = (A_{1,1} + \alpha_{1,1})x_1(t) + (B_{1,1} + \beta_{1,1})u_1(t). \tag{53}$$

Supermarket 2

$$x_2(t+1) = (A_{2,1} + \alpha_{2,1})x_2(t) + (B_{2,1} + \beta_{2,1})u_2(t). \tag{54}$$

Chiller 1

$$x_3(t+1) = \begin{cases} x_3(t) + (B_{3,1} + \beta_{3,1})u_3(t) & u_3(t) \geq 0 \\ x_3(t) + (B_{3,2} + \beta_{3,2})u_3(t) & u_3(t) < 0. \end{cases} \tag{55}$$

Chiller 2

$$x_4(t+1) = \begin{cases} x_4(t) + (B_{4,1} + \beta_{4,1})u_4(t) & u_4(t) \geq 0 \\ x_4(t) + (B_{4,2} + \beta_{4,2})u_4(t) & u_4(t) < 0. \end{cases} \tag{56}$$

A. Heterogeneous Versus Homogeneous Aggregation: Performance Comparison

The setup consists of two aggregators. In the homogeneous setup, "Aggregator 1" controls the supermarkets and "Aggregator 2" controls the chillers. In the heterogeneous setup, "Supermarket 1" and "Chiller 1" are under the control of the "Aggregator 1," "Supermarket 2" and "Chiller 2" are under the control of the "Aggregator 2." In this part, we assume fixed model parameters for the consumers. As we discussed above, we consider a two-level optimization problem, a static optimization and a dynamic optimization, which provide the optimum power distribution from the top-level controller to the aggregators and from each aggregator to the connected consumers, respectively. For the static optimization, each aggregator needs to communicate the cost/profit curves, per a specified power reference, for up/down-regulating scenarios. Fig. 4 shows these curves for our simulation models. Depending on the consumer type, each aggregator can offer different power ranges to follow in homogeneous and heterogeneous setup. For instance, the supermarkets have less

This article has been accepted for inclusion in a future issue of this journal. Content is final as presented, with the exception of pagination.

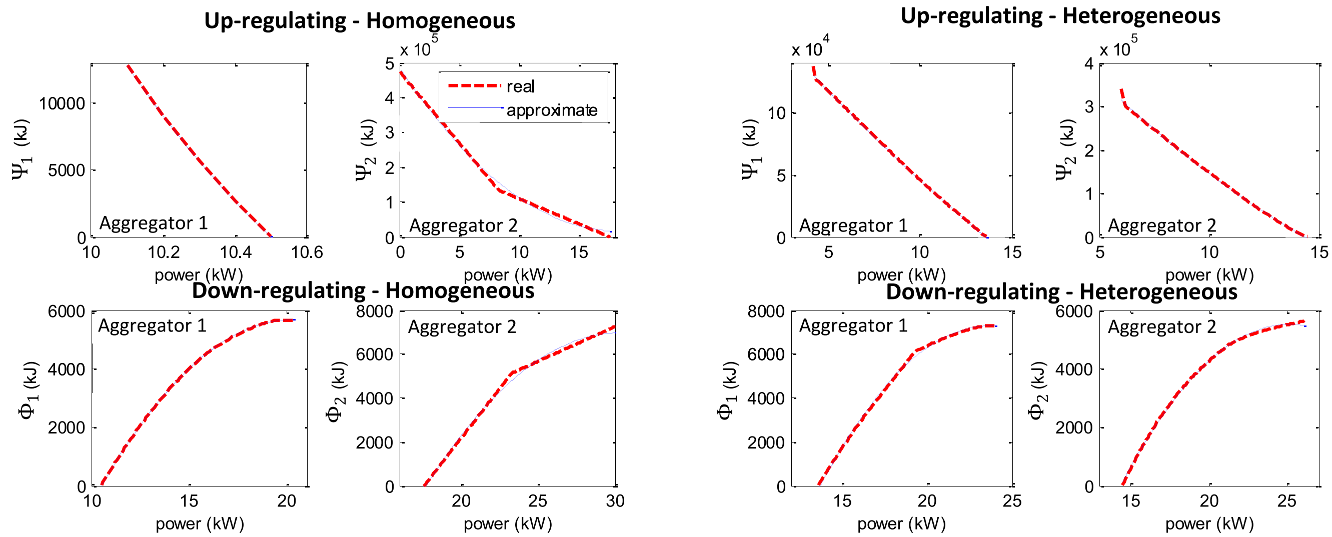

Fig. 4. Top: cost curves (extra energy consumption) that are communicated by each aggregator in up-regulating scenario while bottom: profit curves (extra energy saving) in down-regulating scenario. The left figures are related to the homogeneous setup while the right figure are related to the heterogeneous setup. The real communicated values are shown with dashed red lines while the blue solid lines show the fitted second order polynomial.

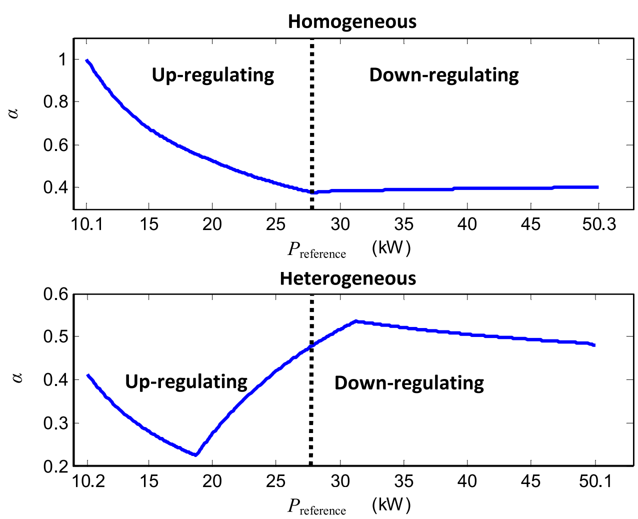

Fig. 5. Static optimization at the top-level controller: $\alpha = (P_1/P_{\text{reference}})$, where P_1 is the input power to the "Aggregator 1" and $P_{\text{reference}}$ is the input power to the top-level controller. Top: optimum value of α for the homogeneous setup while bottom: for the heterogeneous one.

capacity compared to the ice storages in our simulation examples. That is why the aggregator with just the supermarkets offers a smaller range of power to follow. In order to use these values in the optimization (32)–(35), we fit the curves with second order polynomials, shown with the blue solid lines.

There are two aggregators in the setup, $n = 2$. Thus the top-level controller should provide P_1 and P_2 from the static optimization, which are the input power to each aggregator. Fig. 5 shows the results of the optimization at the top-level controller, where α indicates the ratio of the power of the first aggregator to the power reference that the top-level controller is asked to follow. Therefore, we have

$$P_1 = \alpha P_{\text{reference}} \tag{57}$$

$$P_2 = (1 - \alpha) P_{\text{reference}}. \tag{58}$$

The homogeneous setup can follow a greater range of power, [10.1–50.3 kW], compared to the heterogeneous setup, [10.2–50.1 kW]. However, the difference is not significant. The baseline power of the whole portfolio is $P_{\text{base}} = 28.1$ kW, which is shown with the dashed line to distinguish the up-regulating and down-regulating scenarios. Again, the value of α for each setup and for each scenario depends on the consumer characteristics. For instance, assume the heterogeneous setup and up-regulating scenario. In the beginning, α decreases as the deviation from baseline power increases. This means the use of "Aggregator 1" increases since P_1 decreases and "Aggregator 1" needs to reduce its consumption more than before. However, for $P_{\text{reference}} = 18.7$ kW, $\alpha = 0.2246$, and then $P_1 = 4.2$ kW. This is the minimum power that can be followed by "Aggregator 1" in heterogeneous, up-regulating scenario. Thus, α should increase as the deviation increases from this place in order to keep P_1 at 4.2 kW.

During the time of activation, a dynamic optimization is run at each aggregator every sampling time to define the optimum power distribution from the aggregators to the relevant consumers. Above, we can see the results of the dynamic optimization for some fixed model parameters in a 1-h activation time. For each up-regulating and down-regulating scenario, we consider two power references to show the results of large and small deviation from the baseline power. In addition to power distributions, the thermal energy changes are also shown. Fig. 6 illustrates the heterogeneous setup. As we can see, for small deviations from the baseline ($P_{\text{reference}} = 26$ kW and $P_{\text{reference}} = 31$ kW), only "Aggregator 1" is utilized in both up-regulating and down-regulating scenarios. However, for large deviations from the baseline ($P_{\text{reference}} = 15$ kW and $P_{\text{reference}} = 42$ kW), both aggregators are required to change their consumption. In our simulation examples, "Supermarket 1" has a higher COP than "Supermarket 2." Although "Supermarket 1" has a higher heat loss than "Supermarket 2," the difference in

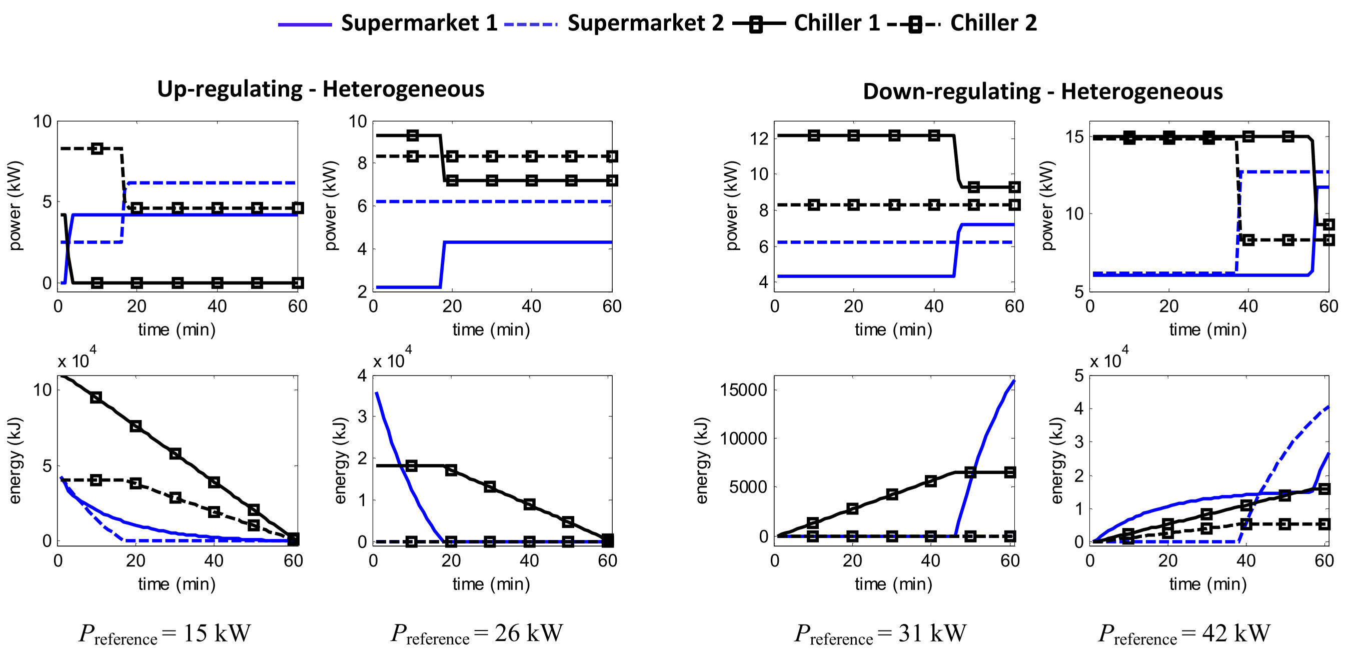

Fig. 6. Dynamic optimization at the aggregators for the heterogeneous setup. Top: power distributions for the four consumers for different power references and bottom: associated thermal energy changes during a 1-h activation time.

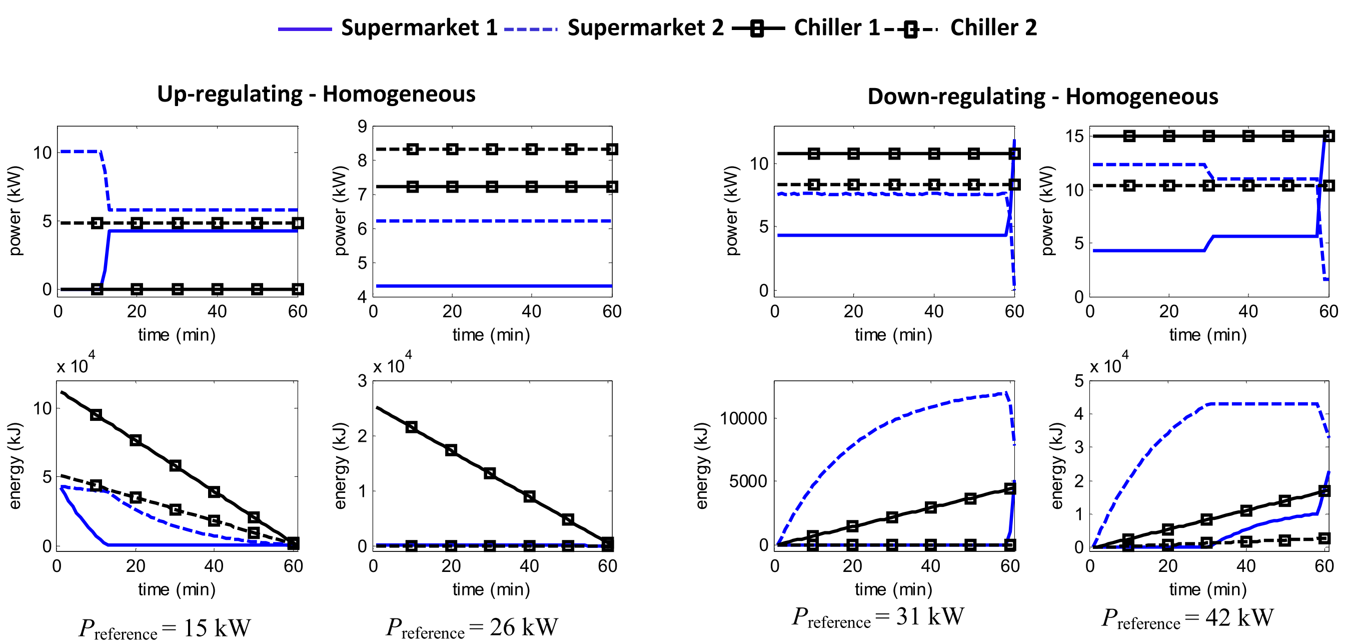

Fig. 7. Dynamic optimization at the aggregators for the homogeneous setup. Top: power distributions for the four consumers for different power references and bottom: associated thermal energy changes during a 1-h activation time.

COPs are more important for our examples. On the other hand, "Chiller 2" is more efficient than "Chiller 1" since it has a lower difference between the two COPs of cooling and charging modes. Thus, the combination of "Supermarket 1" and "Chiller 2" is more efficient than the other two. Another thing that can be seen is that there is a switching between the supermarket and the chiller which are connected to each aggregator in such a way that the supermarket is mostly utilized in the beginning in the up-regulating and at the end in the down-regulating scenarios. This is reasonable due to the leaky nature of the supermarket. Fig. 7 shows the results for the homogeneous setup. Again, different power distributions can be seen for different power references. Between the two supermarkets of "Aggregator 1," there could be several switchings depending on the system dynamics. For instance, for $P_{\text{reference}} = 15$ kW, "Supermarket 1" is utilized first due to the higher heat loss than "Supermarket 2," while for $P_{\text{reference}} = 42$ kW, "Supermarket 2" is utilized first for the same reason. Between the two chillers of "Aggregator 2," the one ("Chiller 1" in our example) with the higher ratio of

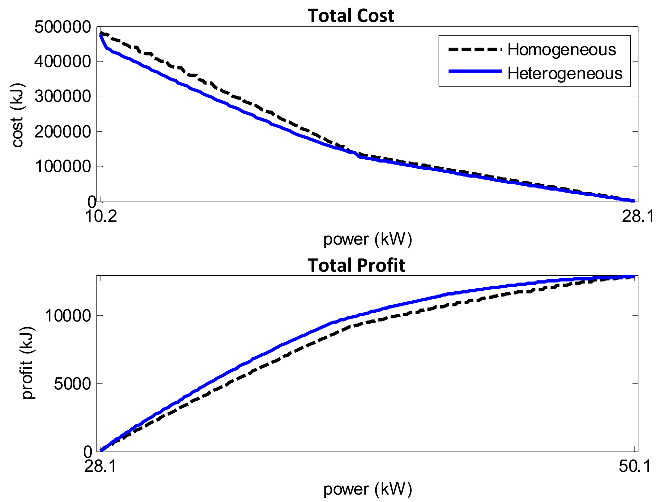

Fig. 8. Total cost (extra energy consumption) and total profit (extra energy saving) for the homogeneous and heterogeneous setup.

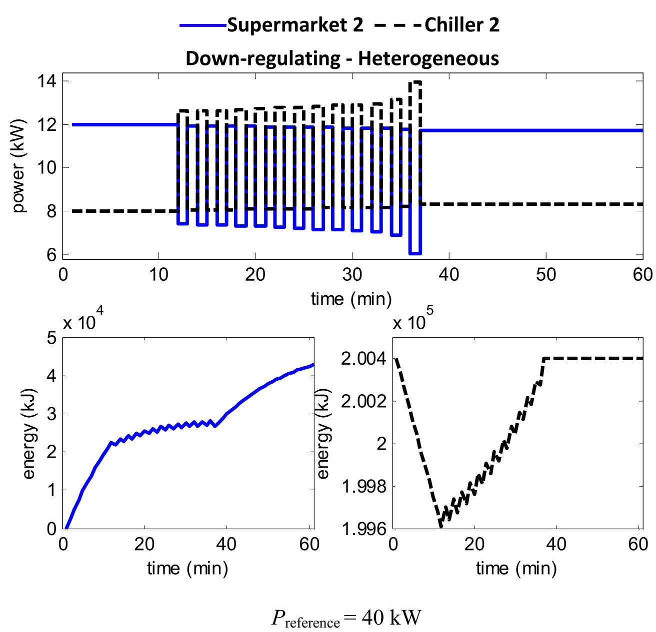

Fig. 9. Power distributions and thermal energy changes for the heterogeneous setup with two identical supermarkets and chillers and down-regulating scenario. The both ice storages are fully charged at the beginning of activation time.

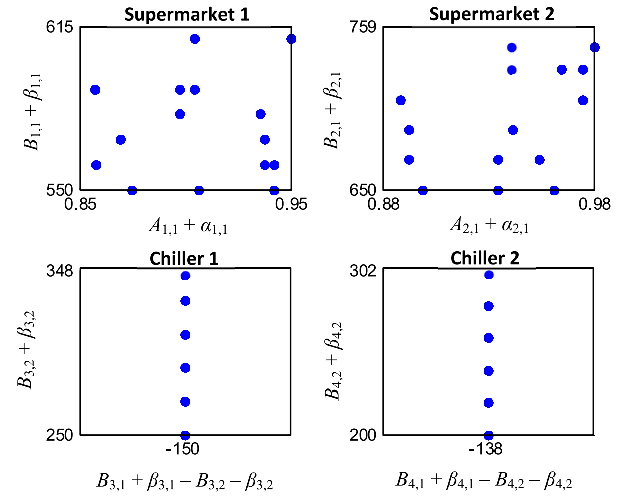

Fig. 10. Uncertainty set of the model parameters for the up-regulating scenario.

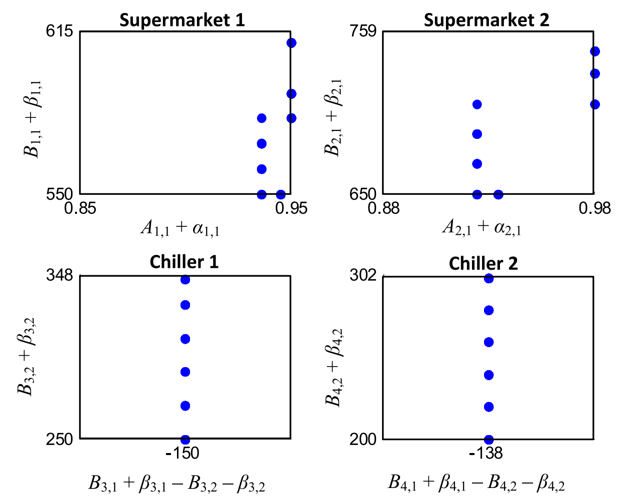

Fig. 11. Uncertainty set of the model parameters for the down-regulating scenario.

($\mathrm{COP}_{\text{charging}}/\mathrm{COP}_{\text{cooling}}$) is utilized first as long as there is ice in the tank and the maximum power is not reached. After that, the second chiller becomes active.

Total profit and total cost for the whole range of power reference are shown in Fig. 8. The heterogeneous setup has lower cost and higher profit compared to the homogeneous setup. The difference is greater for larger deviations from the baseline.

We assumed that the consumers are naturally available to increase their power consumption. In above simulations, we assumed the temperature of cold rooms and display cases at the supermarket are normally kept at the maximum level in order to reduce power consumption. Moreover, there is also enough space at the ice tank in normal situation. Let us consider a situation in which the both ice tanks are fully charged at the beginning of activation time. Fig. 9 shows the result of simulating this situation for the heterogeneous setup, where we assume two identical supermarkets and chillers ("Supermarket 2" and "Chiller 2" in our examples) in order to eliminate the power distribution problem from the top-level controller to the aggregators. Hence, each aggregator receives ($P_{\text{reference}}/2$) to follow. The top-level controller should follow $P_{\text{reference}} = 40$ kW during a 1-h activation time while the $P_{\text{base}} = 29$ kW. Thus, the service is down-regulating. The chiller is not able to consume more than its baseline, 8.3 kW, since the ice tank is fully charged and the supermarket cannot consume the rest of power, 11.7 kW, for 1 h since the minimum temperature of the cold rooms will be violated. The heterogeneous aggregator can handle this situation in this way: in the beginning of activation time, the chiller consumes a little bit below its baseline power. So, it needs to melt some ice to provide the cooling load from the building. Melting ice

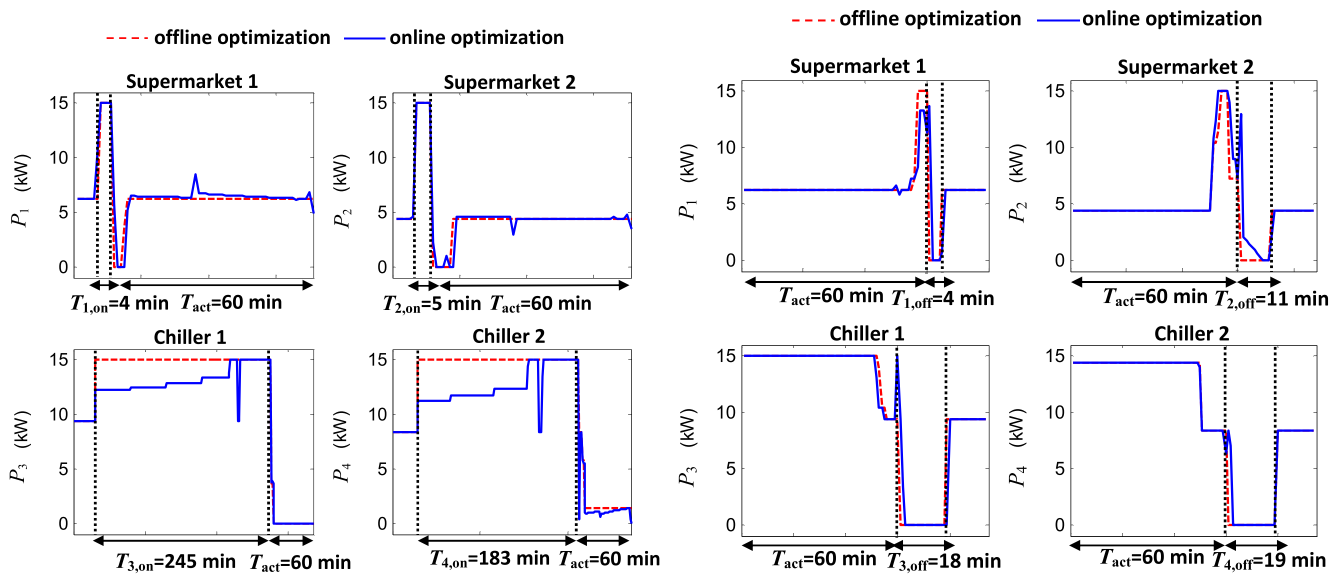

Fig. 12. Robust MPC setup. The four figures on the left show the power distributions in the up-regulating scenario and the four figures on the right show the power distributions in the down-regulating scenario during the extended activation time.

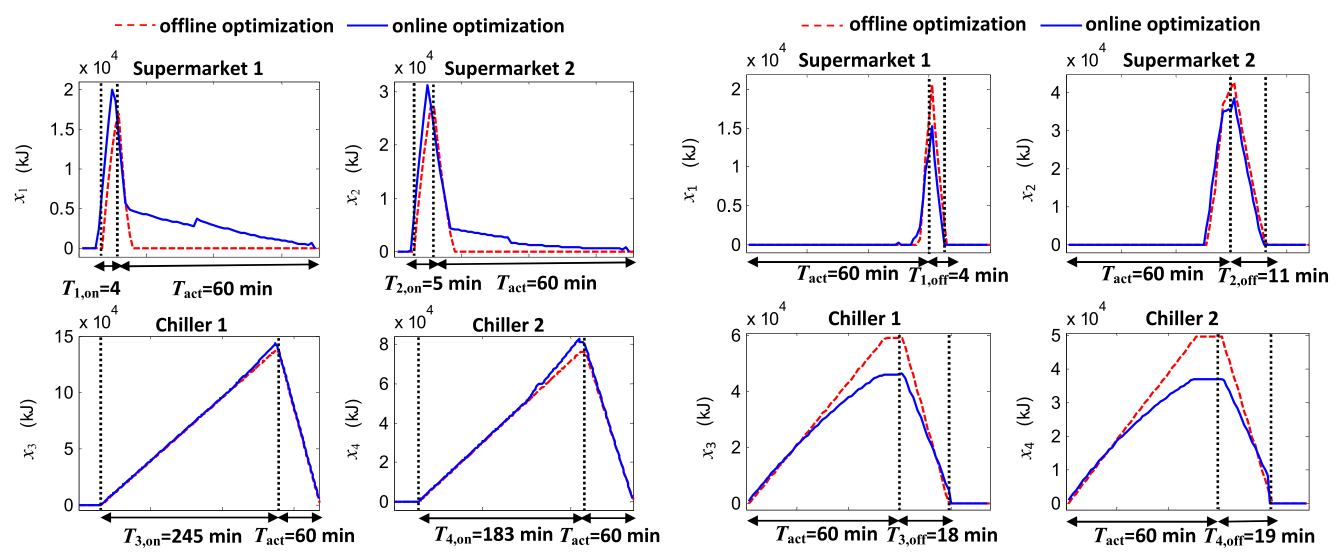

Fig. 13. Robust MPC setup. The four figures on the left show the thermal energy changes in the up-regulating scenario and the four figures on the right show the thermal energy changes in the down-regulating scenario during the extended activation time.

in this period provides some space in the ice tank. Then the chiller is able to consume above its baseline and the supermarket can decrease its consumption to decrease the rate of energy saving. As we can see, several switchings occur between the supermarket and chiller during the ice building period. At the end of the activation time, we again have a fully charged ice tank. This flexibility is not available in the homogeneous setup.

B. Robust MPC

The setup consists of one aggregator which controls two supermarkets and two chillers. In this part, we examine the effect of changes in model parameters and the proposed robust MPC setup. Uncertainty sets of the system parameters for the up-regulating and the down-regulating scenarios are shown in Figs. 10 and 11. For the supermarkets, we assume that the parameters $A_{1,1}$ and $A_{2,1}$ are changed randomly every 30 min, since these parameters describe the heat loss to the surrounding and are dependent on the customers' behavior at the supermarkets. $B_{1,1}$ and $B_{2,1}$ reflect the COP of the compressors. We assume these parameters decrease during the activation time, since the consumers are operated outside of their optimum region. For the chillers, $B_{3,1}$ and $B_{4,1}$ represent the COP in charging mode ($\mathrm{COP}_{\mathrm{charging}}$), whereas $B_{3,2}$ and $B_{4,2}$ reflect the COP in cooling mode ($\mathrm{COP}_{\mathrm{cooling}}$). We also assume these parameters decrease during the activation with the same rate, such that the differences ($B_{3,1} + \beta_{3,1} - B_{3,2} - \beta_{3,2}$ and $B_{4,1} + \beta_{4,1} - B_{4,2} - \beta_{4,2}$) which appear in the final models, are fixed.

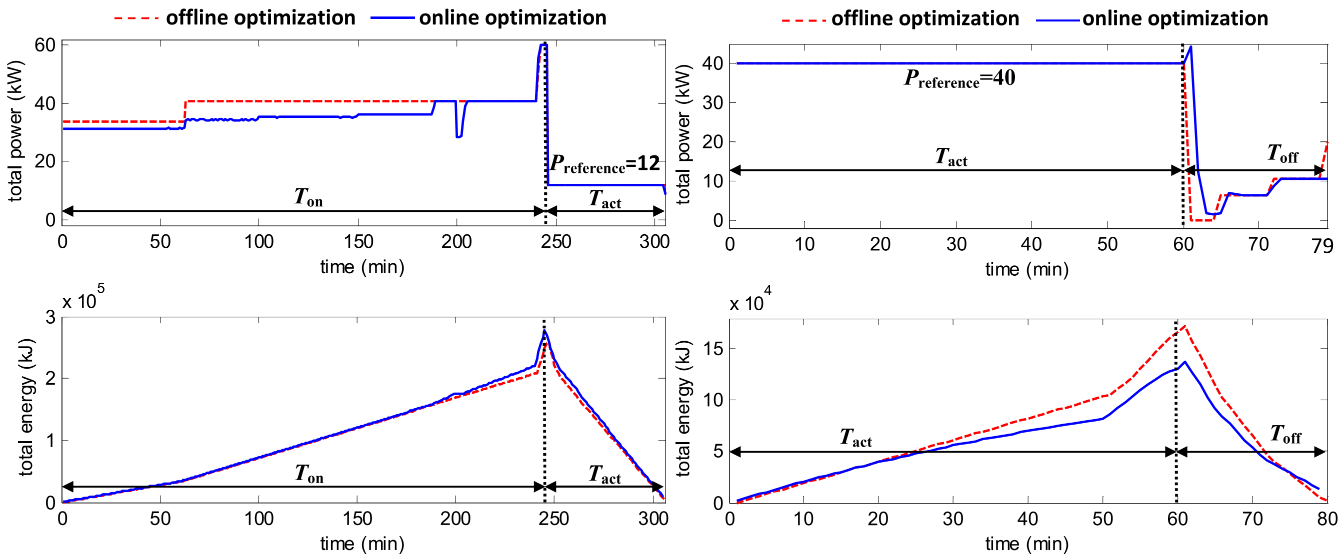

Fig. 14. Robust MPC setup. The left figures show total power and total energy during the activation time plus the maximum on-time period of the four consumers (T_{on}) in the up-regulating scenario and the right figures show total power and total energy during the activation time plus the maximum off-time period of the four consumers (T_{off}) in the down-regulating scenario.

Simulation results for the up-regulating and down-regulating scenarios for $P_{\text{reference}} = 12$ kW and $P_{\text{reference}} = 40$ kW are depicted below. Figs. 12 and 13 show the electrical power and the thermal energy changes of each consumer during the extended activation time, respectively. The red dashed lines are the desired values, which are obtained from the offline optimization with the fixed model parameters long before the activation time, whereas the blue solid lines are the real values during the service activation, when the model parameters are time-varying. As we described earlier, an online optimization is run during the service activation which aims to minimize the deviation between the desired and real values with a quadratic cost function. On-time and off-time periods of each consumers are also shown in the figures. The chillers have quite longer on-time periods in the up-regulating scenario compared to the supermarkets for our simulation examples. The difference between the desired and real power is also greater for the chillers in up-regulation.

Total electrical power and thermal energy changes of the four consumers are shown in Fig. 14. The values are shown during $T_{\text{act}} + T_{\text{on}}$ for the up-regulating scenario and during $T_{\text{act}} + T_{\text{off}}$ for the down-regulating scenario, where T_{on} is the maximum on-time period and T_{off} is the maximum off-time period of the four consumers. T_{act} denotes the activation time. The results are as we expected. In both scenarios, the aggregated power consumption is equal to $P_{\text{reference}}$ during T_{act}. For the up-regulating scenario, the actual power consumption is lower than the value which is obtained from the offline optimization. This is reasonable since the offline optimization has been performed for the worst case in which the cost is maximum. However, the situation is better during the service activation and accordingly, lower energy consumption is needed during T_{on}. On the other hand, in the down-regulating scenario, the offline optimization has been performed for the best case in which the profit is maximum. That is why the power consumption is above the offline value during the off-time period, which means the lower profit.

V. Conclusion

This paper proposes a three-level hierarchical structure to employ the flexibility of industrial thermal loads in the future electricity market. The setup consists of a top-level controller which is located at the grid operator (BRP, TSO, or DSO) and a set of aggregators, each of which controls a number of consumers. Based on a contract agreement, each aggregator is asked by the top-level controller to follow a specified power during an activation time. Likewise, the aggregator is given a permission to send power references to the consumers. We consider an optimal controller at the top-level which receives cost/profit curves per a specified power reference. Having this information, it provides the optimal power distribution. At the aggregator, a robust MPC is considered for optimal power distribution. The aggregator requires a model of consumption units to run the optimization. In this paper, we assume a piece-wise linear model for the industrial thermal loads.

Simulation of the proposed robust MPC for our particular case studies reveals that the robust design can handle the mismatch between the actual and assumed model of consumers pretty well. Moreover, we consider two types of aggregation: 1) homogeneous aggregation in which each aggregator controls the same consumer type; and 2) heterogeneous aggregation in which each aggregator controls a heterogeneous portfolio of consumers. Simulation results for the two different consumers, supermarket and chiller, shows the heterogeneous aggregation outperforms the homogeneous one. First, the heterogeneous aggregation has a lower cost and greater profit from energy consumption point of view. Second, unpredictable situations can be better handled with the heterogeneous aggregation. In other words, the heterogeneous aggregation is more flexible than the homogeneous one.

Future work involves testing the proposed strategy on actual commercial consumers.

References

[1] G. M. Shafiullah, A. M. T. Oo, D. Jarvis, A. B. M. S. Ali, and P. Wolfs, "Potential challenges: Integrating renewable energy with the smart grid," in *Proc. 20th Australian Univ. Power Eng. Conf. (AUPEC)*, Christchurch, New Zealand, Dec. 2010, pp. 1–6.

[2] P. B. Andersen, J. Hu, and K. Heussen, "Coordination strategies for distribution grid congestion management in a multi-actor, multi-objective setting," in *Proc. 3rd IEEE PES Int. Conf. Exhibit. Innov. Smart Grid Technol. (ISGT)*, Berlin, Germany, Oct. 2012, pp. 1–8.

[3] V. C. Gungor *et al.*, "Smart grid technologies: Communication technologies and standards," *IEEE Trans. Ind. Informat.*, vol. 7, no. 4, pp. 529–539, Nov. 2011.

[4] X. Fang, S. Misra, G. Xue, and D. Yang, "Smart grid—The new and improved power grid: A survey," *IEEE Commun. Surveys Tuts.*, vol. 14, no. 4, pp. 944–980, Oct. 2012.

[5] D. York and M. Kushler, "Exploring the relationship between demand response and energy efficiency: A review of experience and discussion of key issues," Amer. Council Energy-Efficient Econ., Washington, DC, USA, Tech. Rep. U052, 2005.

[6] M. A. A. Pedrasa, T. D. Spooner, and I. F. MacGill, "Coordinated scheduling of residential distributed energy resources to optimize smart home energy services," *IEEE Trans. Smart Grid*, vol. 1, no. 2, pp. 134–143, Sep. 2010.

[7] M. Tasdighi, H. Ghasemi, and A. Rahimi-Kian, "Residential microgrid scheduling based on smart meters data and temperature dependent thermal load modeling," *IEEE Trans. Smart Grid*, vol. 5, no. 1, pp. 349–357, Jan. 2014.

[8] S. Kishore and L. Snyder, "Control mechanisms for residential electricity demand in smart grids," in *Proc. 1st IEEE Int. Conf. Smart Grid Commun.*, Gaithersburg, MD, USA, Oct. 2010, pp. 443–448.

[9] Y. Ma, A. Kelman, A. Daly, and F. Borrelli, "Predictive control for energy efficient buildings with thermal storage: Modeling, stimulation, and experiments," *IEEE Control Syst. Mag.*, vol. 32, no. 1, pp. 44–64, Feb. 2012.

[10] Y. Ma *et al.*, "Model predictive control for the operation of building cooling systems," *IEEE Trans. Control Syst. Technol.*, vol. 20, no. 3, pp. 796–803, May 2012.

[11] F. Oldewurtel *et al.*, "Use of model predictive control and weather forecasts for energy efficient building climate control," *Energy Build.*, vol. 45, pp. 15–27, Feb. 2012.

[12] E. Vrettos, K. Laiy, F. Oldewurtel, and G. Andersson, "Predictive control of buildings for demand response with dynamic day-ahead and real-time prices," in *Proc. Eur. Control Conf. (ECC)*, Zurich, Switzerland, Jul. 2013, pp. 2527–2534.

[13] B. Biegel, L. H. Hansen, J. Stoustrup, P. Andersen, and S. Harbo, "Adjustable consumption participating in the electricity markets," in *Proc. IEEE 52nd Annu. Conf. Decis. Control (CDC)*, Florence, Italy, Dec. 2013, pp. 4943–4948.

[14] J. Medina, N. Muller, and I. Roytelman, "Demand response and distribution grid operations: Opportunities and challenges," *IEEE Trans. Smart Grid*, vol. 1, no. 2, pp. 193–198, Sep. 2010.

[15] A. M. Kosek, G. T. Costanzo, H. W. Bindner, and O. Gehrke, "An overview of demand side management control schemes for buildings in smart grids," in *Proc. IEEE Int. Conf. Smart Energy Grid Eng. (SEGE)*, Oshawa, ON, Canada, Aug. 2013, pp. 1–9.

[16] S. Harbo and B. Biegel, "Contracting flexibility services," Dept. Electron. Syst. Autom. Control, Danish Energy Assoc., Frederiksberg, Denmark, Aalborg Univ., Aalborg, Denmark, Tech. Rep. Cross WP2, WP5 iPower project, 2012.

[17] S. Han, S. Han, and K. Sezaki, "Development of an optimal vehicle-to-grid aggregator for frequency regulation," *IEEE Trans. Smart Grid*, vol. 1, no. 1, pp. 65–72, Jun. 2010.

[18] M. A. Lopez, J. A. Aguado, S. de la Torre, and M. Figueroa, "Optimization-based market-clearing procedure with EVs aggregator participation," in *Proc. 4th IEEE PES Innov. Smart Grid Technol. Eur. (ISGT EUROPE)*, Kongens Lyngby, Denmark, Oct. 2013, pp. 1–5.

[19] B. Sanandaji, H. Hao, and K. Poola, "Fast regulation service provision via aggregation of thermostatically controlled loads," in *Proc. 47th Hawaii Int. Conf. Syst. Sci. (HICSS)*, Waikoloa, HI, USA, Jan. 2014, pp. 2388–2397.

[20] H. Hao, B. Sanandaji, K. Poola, and T. Vincent, "Aggregate flexibility of thermostatically controlled loads," *IEEE Trans. Power Syst.*, vol. 30, no. 1, pp. 189–198, Jan. 2014.

[21] J. L. Mathieu, M. Kamgarpour, J. Lygeros, G. Andersson, and D. S. Callaway, "Arbitraging intraday wholesale energy market prices with aggregations of thermostatic loads," *IEEE Trans. Power Syst.*, vol. 30, no. 2, pp. 763–772, Mar. 2015.

[22] S. Bashash and H. K. Fathy, "Modeling and control of aggregate air conditioning loads for robust renewable power management," *IEEE Trans. Control Syst. Technol.*, vol. 21, no. 4, pp. 1318–1327, Jul. 2013.

[23] L. Gkatzikis, I. Koutsopoulos, and T. Salonidis, "The role of aggregators in smart grid demand response markets," *IEEE J. Sel. Areas Commun.*, vol. 31, no. 7, pp. 1247–1257, Jun. 2013.

[24] E. Vrettos, F. Oldewurtel, F. Zhu, and G. Andersson, "Robust provision of frequency reserves by office building aggregations," in *Proc. World Congr. Int. Fed. Autom. Control (IFAC)*, Cape Town, South Africa, Sep. 2014, pp. 12068–12073.

[25] N. Lu, "An evaluation of the HVAC load potential for providing load balancing service," *IEEE Trans. Smart Grid*, vol. 3, no. 3, pp. 1263–1270, Sep. 2012.

[26] S. Rahnama, J. D. Bendtsen, J. Stoustrup, and H. Rasmussen, "Power balancing aggregator design for industrial consumers using direct control," in *Proc. 14th Eur. Control Conf. (ECC)*, Linz, Austria, Jul. 2015.

[27] S. Rahnama, S. E. Shafiei, J. Stoustrup, H. Rasmussen, and J. D. Bendtsen, "Evaluation of aggregators for integration of large-scale consumers in smart grid," in *Proc. IFAC WC*, Cape Town, South Africa, Aug. 2014, pp. 1879–1885.

[28] A. Bemporad and M. Morari, "Control of systems integrating logic, dynamics, and constraints," *Automatica*, vol. 35, no. 3, pp. 407–427, Mar. 1999.

Samira Rahnama received the B.S. degree from the Iran University of science and Technology, Tehran, Iran, in 2006, and the M.S. degree from the Malek-Ashtar University of Technology, Tehran, in 2010, both in electrical engineering (control). She is currently pursuing the Ph.D. degree in control engineering with the Department of Electronic Systems, Automation, and Control, Aalborg University, Aalborg, Denmark.

Her current research interests include smart grid and demand response, predictive control, and optimization.

Jan Dimon Bendtsen (M'11) was born in Denmark, in 1972. He received the M.Sc. degree in electronic engineering and the Ph.D. degree in control engineering from the Department of Electronic Systems, Aalborg University, Aalborg, Denmark, in 1996 and 1999, respectively.

Since 2003, he has been an Associate Professor with the Department of Electronic Systems, Aalborg University. In 2005, he was a Visiting Researcher with the Australian National University, Canberra, ACT, Australia. Since 2006, he has been involved in the management of several national and international research projects, and organizing international conferences. In 2012 and 2013, he was a Visiting Researcher with the University of California, San Diego, CA, USA. His current research interests include adaptive control of nonlinear systems, closed loop system identification, control of energy systems, and infinite-dimensional systems.

Dr. Bendtsen was a co-recipient of the Best Technical Paper Award at the American Institute of Aeronautics and Astronautics Guidance, Navigation, and Control Conference in 2009.

Jakob Stoustrup (S'89–M'91–SM'99) received the M.Sc. degree in electrical engineering and the Ph.D. degree in applied mathematics from the Technical University of Denmark, Kongens Lyngby, Denmark, in 1987 and 1991, respectively.

From 1991 to 1996, he held several positions with the Department of Mathematics, Technical University of Denmark, and he was a Visiting Professor with the University of Strathclyde, Glasgow, U.K., and Mittag-Leffler Institute, Stockholm, Sweden. From 1997 to 2013, he was a Professor of Automation and Control, and since 2006, he has been the Head of Research with the Department of Electronic Systems, Aalborg University, Aalborg, Denmark. Since 2014, he has been the Chief Scientist with Pacific Northwest National Laboratory, Richland, WA, USA, leading the control of complex systems initiative for the U.S. Department of Energy. His main contributions have been to robust control theory and to the theory of fault tolerant control systems. With co-workers, he has proposed a novel plug-and-play control framework. Apart from the theoretical work, he has been involved in applications in cooperation with 100+ industrial companies, including acting as the Chief Executive Officer for two technological startup companies. He has published approximately 300 peer-reviewed scientific papers with an H-index of 30.

Dr. Stoustrup was a recipient of the Statoil Prize, the Dannin Award for Scientific Research, several conference paper awards, and the Chivalric Order of the Dannebrog for his research contributions. He was an Associate Editor and an Editorial Board Member of several international journals. He served as the General Chair, the Program Chair, and an International Program Committee Member for several international conferences. He has been the Chairman of the IEEE Control System Society (CSS)/Robotics and Automation Society Joint Chapter. He was the Chair of the IEEE CSS Technical Committee on Smart Grids. In 2013, he was appointed as the first IEEE CSS Wikipedia Editor. He was the Chair of the International Federation of Automatic Control (IFAC) Technical Committee Symposium on Fault Detection, Supervision, and Safety for Technical Processes, and a Member of the IFAC Technical Board. He was a Member of the European Research Council, as well as the Danish, Norwegian, and Swedish Research Councils. He is a Member of the Danish Academy of Technical Sciences, where he has acted as a Board Member.

Henrik Rasmussen was born in Denmark, in 1944. He received the M.Sc. degree from Danish Technical University, Kongens Lyngby, Denmark, in 1970, with specialization in electro physics, and the Ph.D. degree in control engineering from the Department of Electronic Systems, Aalborg University, Aalborg, Denmark, in 1996.

He was an Associate Professor with Aalborg University, until 2012 where he retired.